

Is an Image Also Worth $16 \times 16 = 256$ Superpixels? A Framework for Attentional Image Classification

Pedro Henrique da Costa Avelar^{*,ufrgs,uom}, Anderson R. Tavares^{ufrgs}, and Luís C. Lamb^{ufrgs}

^{ufrgs}Institute of Informatics, Federal University of Rio Grande do Sul (UFRGS), 91501-970, Porto Alegre, Rio Grande do Sul, Brazil

^{uom}Division of Informatics, School of Health Sciences, Imaging and Data Science, Faculty of Biology, Medicine and Health, University of Manchester, M13 9GB, Vaughan House, Portsmouth St, Manchester, United Kingdom

Abstract

Superpixel-based image classification has traditionally leveraged graph neural networks (GNNs) for processing irregular image representations. Recent advances in computer vision, driven by Vision Transformers (ViTs), have introduced new paradigms in self-attentional models, surpassing convolutional neural networks (CNNs) in various tasks. However, a synergistic connection between GNNs, superpixels, and transformers remains unexplored. In this work, we propose Superpixel Transformers (SPT), a novel framework that unifies superpixel-based image classification and ViTs. SPT generalizes the Superpixel Image Classification with Graph Attention Networks (SICGAT) model and ViT to support arbitrary superpixel-based chunking strategies, connectivity graphs, and positional encodings. We introduce refinements including a multidimensional sine-cosine positional encoding and an enriched patch data structure that fully incorporates superpixel shape and color information. By testing SPT across datasets such as CIFAR10, FashionMNIST, and Imagenette, with various superpixel generation and graph connectivity strategies, we demonstrate that SPT achieves superior performance compared to previous superpixel-based GNN methods and remains competitive with ViTs. Notably, our approach addresses the limitations of SICGAT, such as information loss during pixel aggregation, and shows how constrained graph connectivity can enhance ViT performance. SPT bridges the gap between superpixel-based and transformer models, opening avenues for

cross-domain generalization and future innovations in hybrid attentional frameworks, and showing that an image can also be worth 16×16 superpixels.

1 Introduction

Although superpixel-like segmentation algorithms have been used together with Neural Networks for processing images since 2005 [9], it was only in 2017 that modern iterations of Graph Neural Networks started using superpixel algorithms to generate image graphs [28]. This scheme has been worked on and improved throughout many iterations throughout the years. In particular, using a Graph Neural Network kernel with an attentional mechanism [4] greatly improved performance from previous works even when using a more restrictive adjacency matrix, which the authors claim makes the problem harder to solve.

Shortly after this development of using attention mechanisms and Superpixels for image processing, the uncontested leadership of Convolutional Neural Networks (CNNs) in Computer Vision was upended by another attention-based approach: Vision Transformers [16]. Vision Transformers have since become a staple in Computer Vision and, despite being notoriously data-hungry, they have surpassed CNNs in many applications, including image classification, object detection and semantic image segmentation [34].

To the best of our knowledge, no previous work has yet linked Vision Transformers with GNN- and Superpixel-based image classification. In this paper we will bridge the gap between Superpixel Image Classification and Vision Transformers and put

*This work was developed entirely at UFRGS.

them into a framework of attentional image classification. We attempt to ablate which components are crucial for better performance and generalisability in an attempt to challenge the notion that Graph Neural Networks cannot be deep and unify both fields.

We do so by proposing a framework that generalises both the Superpixel Image Classification with Graph Attention Networks (SICGAT) model proposed in [5] as well as the Vision Transformer (ViT) model [16], while providing a framework that can work with multiple patch types and allowing for arbitrary graph connectivities. We include tests with both grid-patches like in ViT and also extend SICGAT’s superpixels into a patch-like data-structure that fully utilises the information from both the superpixel’s shape as well as the colour information of each component superpixel. We test our models with three common graph strategies from the literature [28, 5, 16, 30] and show that Vision Transformers might benefit from a more constrained connectivity graph between its patches. Finally, we propose an extension of the Sine-Cosine positional embedding from [38] to an arbitrary number of dimensions, which we show to be highly beneficial for working in a superpixel environment. We hope that these developments will allow the areas of Superpixel Image Classification to be unified with those of mainstream Computer Vision and that these models spur further investigation on different superpixel formats for future ViT work.

2 Background

2.1 Image superpixels

Superpixels are groups of pixels in semantically similar areas of an image. A number of techniques exist to generate superpixels from images, such as SLIC [1], SNIC [3], SEEDS [37], ETPS [47], and SH [42]. Out of these techniques, SLIC is widely thought of as one of the most stable and is still recommended over other state-of-the-art algorithms [35].

SLIC is a modified version of the k-means clustering algorithm, which only attempts to assign points to cluster centroids if these points are inside a $2S$ -sized square centred in the centroid, where $S = N/k$, with N being the number of pixels in the image and k the desired number of superpixels. It works by initialising k cluster means C_j composed of a colour component c_{C_j} and a spatial component s_{C_j} , and then iteratively assigning pixels to clusters, and updating the cluster means based on their component

pixels. Distances between cluster means and respective pixels are calculated as the L2 norm of the two normalised Euclidean distance vectors: one for the colour component and one for the spatial component, normalised by the expected maximum spatial distance (S) and the maximum expected colour distance, which is usually represented by a manually-selected constant m^2 .

While the usual representation for images – a grid/tensor of pixels – can already be seen as a regular grid graph (a lattice), superpixels induce a more natural graph representation of an image [28, 5]. This is due to the fact that, since superpixels are usually irregular, the connectivity between superpixels requires a more abstract structure than a simple grid or hypercube. Thus, superpixels which have bordering pixels become connected between themselves. Therefore, a superpixel-based representation is more suitable for processing with Graph Neural Networks (Section 2.2).

2.2 Graph Neural Networks

Graph Neural Networks (GNNs), pioneered by [31], have had considerable impact on Machine Learning [7]. This is due, in part, to the Graph Convolutional Network of [25], which made GNNs accessible in modern deep learning frameworks. This has been followed shortly by demonstrations of the power of GNN to model inductive biases of a problem by carefully crafting graphs that matched the structure of the problem [19, 7]. A notable example in this line was the development of NeuroSAT, which modelled a boolean satisfiability (SAT) instance into a bipartite graph between literals and clauses, allowing communication to flow between these iteratively until the neural “solver” reaches equilibrium [33].

GNNs can be interpreted through many different lenses, of which the most common are either a generalization of convolutions and convolutional neural networks [28, 25, 18], or by interpreting GNNs as what are called “Message-Passing Neural Networks” (MPNN) [19, 33]. In summary, under the MPNN framework, a simple graph neural network will receive a graph $G = \{V, E\}$ composed of a set of vertices $v \in V$ and edges $e \in E$, with edges connecting a source $s \in V$ and a target node $t \in V$ $e = (s, t)$. The neural network will first embed the attributes of each of the nodes through a usually learned function so that we have $x_v^0 = f(v)$ and then propagate the information between the nodes using the adjacencies defined through the edges. Under the MPNN

framework, this is seen as each of the nodes u being a neural computer g with state x_u which then exchanges messages $m_u^t = g^t(x_u^t)$ at a discrete time step t (which can also be interpreted as a layer). These messages then are aggregated through some, usually order-invariant, function a on the node’s neighbourhood $N(u)$ to form the basis of the next time steps’ state $x_u^{t+1} = a(\{m_v^{t+1}, v \in N(u)\})$

2.3 Self-attention in Sequences, Images and Graphs

Self-attention establishes connections between different positions of a sequence or set to construct representations, and one of the most successful earlier applications was to provide a learned mapping from sentences between different languages during machine translation [6]. This approach was then successfully applied in many different tasks, including providing approximations to NP-Complete problems such the Travelling Salesperson Problem [40]. However, most of these earlier methods still used other architectural patterns, mostly RNNs, whose input was mediated through attention.

Soon after the development of self-attentional mechanisms to mediate the sequences generated through RNNs, the development of the Transformer model [38] showcased the power behind attentional mechanisms. The Transformer exclusively uses self-attention to mediate the exchange of information between elements of a sequence, which mitigated common RNN issues, such as challenges with long-time dependencies [32, 20] and the inherent lack of parallelism [38]. This new architectural pattern has then been widely adopted and has had applications ranging from Natural Language Processing [29], to Computational Chemistry [43, 21, 41], Computational Biology [11, 13] and, of course, has also recently been widely applied in image processing through the development of the Vision Transformer [16].

The self-attention mechanism in text-based networks are often mediated both through a positional embedding, as well as an attention mask which limits which values in the sequence an element can attend to. The original Transformer, due to its language model purpose, limits the attention mechanism so that elements can only attend to those before it, and uses a Sine-Cosine expansion depending on the position of the element in the sequence to help the attention heads to identify the distance between two attended elements. Another option which also became

widespread was that of using Bidirectional Encoder Representations from Transformers (BERT) [15], allowing all elements to attend to all others, and using a learned positional embedding instead, which was deemed more appropriate for the vision context and used in the Vision Transformer paper [16].

2.3.1 Graph Attention Networks

Graph Attention Networks (GATs) [39] were originally developed in 2017¹ after a surge of interest in Graph-based neural networks [7] due to in part to the Graph Convolutional Network model [25] making graph neural networks accessible in modern deep learning frameworks. Graph attention networks function in a very similar way to other GNN architectures, except that they mediate the message-passing between neighbours through a self-attention mechanism, allowing the network to learn how to prioritise information flow depending on the each node’s information content. This architecture was further refined to allow for the attentional mechanism to be utilised to a higher potential [10].

Is it possible, however, to draw a relationship between GATs and Transformers. In fact, if we assume that a Transformer’s attention mask can be treated as the adjacency matrix in a GAT, it is clear that both architectures work in a similar way, with a layer transforming each input/node, and then having self-attention mediating the information between non-masked inputs/neighbours. GATs differs from Transformers almost only through the lack of specific layers in the update block, such as residual/skip connections and layer/batch normalisation of the input. This similarity has been exploited to develop graph-specific transformer architectures through adopting a graph-specific positional embedding using Laplacian eigenvectors [17].

3 Related Work

While an image is usually represented as a grid of pixels, as mentioned above, if one were to work using superpixels instead, a graph representation becomes required due to the irregular connectivity patterns between superpixels, and has been widely used together with Graph Neural Networks for Superpixel Image Classification [28, 18, 5, 30]. However, to allow for such general connectivity patterns, GNN-based

¹Arxiv version released in 2017 <https://arxiv.org/abs/1710.10903>

methods often aggregate a node’s neighbourhood using the same weight for every neighbour. This implies that simple GNNs would have a lower representational power than convolutional neural networks, since CNNs allow for a different weight to be used for each value in the “neighbourhood” (the convolution window). In fact, a pixel-grid-based GNN was tested in [28] and had a worse performance than a CNN.

The model presented in Superpixel Image Classification with Graph Attention Networks, here onwards referred to as SICGAT, [5] expanded on previous work to allow for a GNN that enables a pseudo-convolutional representational power. This was achieved through using multiple attention heads to mediate the information transfer between nodes in a graph, which allows different “soft”-weights to be learned by the network when aggregating between neighbourhoods. Surprisingly, however, the performance of these models reached its limit with a much smaller amount of attention heads than the medium connectivity in the superpixel graph they built (which is a Region Adjacency Graph). In this paper we will provide a generalisation of their method and show that our model has better results even than their “hard” baseline of using a VGG architecture that only has access to a superpixel-segmented image where each superpixel’s pixels have their RGB values set to their common average. Our model also overcomes the information loss they show in Figure 3.

Recently there has also been a comparative study on the best graph construction method for GCNs [30], which showed an improved performance on [5]’s work even when using a GNN with a lower representational power [46]. They provide a thorough study showing an ablation of various parameters used to build a GNN for SIC and argue that performance was capped at very shallow layer-depths. In this paper we will also perform a thorough exploration of an attention-based GNN model which, thus, has a higher representational power than GCNs and is at least as powerful as a Weissfeiler-Lehman test [46]. Through our ablation, we show that, although more layers did not always cause better performance, the layer depth of our best-performing model often reached our cap for the number of layers (12), which allows for networks four times as deep as the ones used in (author?) [5] and (author?) [30].

4 Superpixel Transformers: A General Framework for Attentional Learning in Images

In this section we provide the definition of our model that generalises the SICGAT model the ViT architecture. We first start by providing a step-by-step description of the differences between SICGAT and the ViT architectures, and then we follow with a description of a concrete formalisation of our model.

4.1 Key differences between Superpixel Image Classification and Vision Transformers

Figure 1 shows a comparison of the SICGAT and ViT architectures. From this, we identify the main differences between these two approaches: (1) Chunking strategy, (2) pixel information aggregation, (3) positional embeddings, (4) architectural differences between a GAT and a Transformer block, (5) differences in chunk connectivity, and (6) pooling vs virtual classification node. We discuss in depth each of these differences next.

Chunking Strategy The first and most obvious difference between the two models is the fact that while SICGAT uses a superpixel algorithm to chunk the image into superpixels, ViT chunks images into equally-sized rectangles. However, this scheme had also previously been used in other superpixel image classification algorithms, such as in MoNET [28], and the approach followed by SICGAT could easily be adapted to also use equally sized chunks. The main reason, however, why SICGAT performs better when chunking the image into superpixels instead of regular patches is due to the pixel information aggregation scheme.

Pixel Information Aggregation Most superpixel image classification methods aggregated the information from all of a chunk’s pixels into a single value, such as taking the average value of pixel intensities around the pixel. This was also followed by SICGAT, and it was shown to cause heavy information loss, as can be seen in Figure 3. ViTs mitigate this by making a linear projection of the flattened pixel inputs for each chunk, which allows the network to learn to use the information from every pixel in a chunk, mitigating the information loss present in SICGAT and other methods such as MoNet.

Positional Embeddings Another difference be-

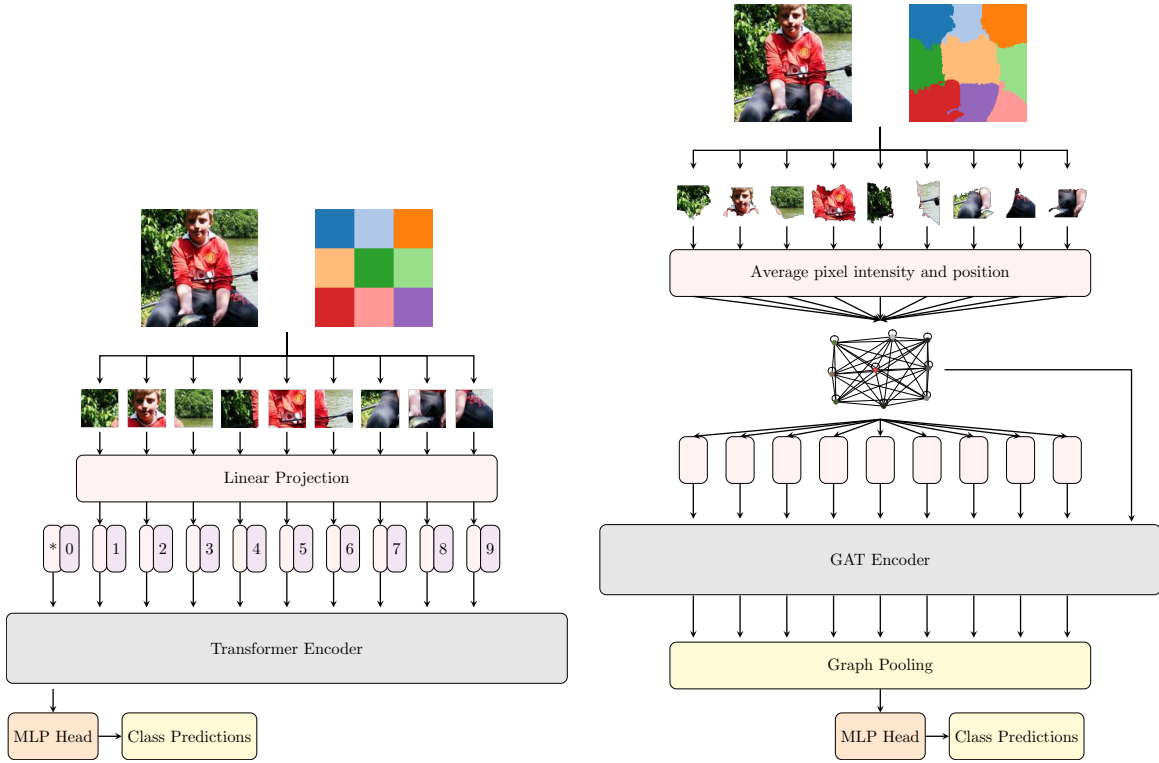


Figure 1: The ViT architecture [16] (left) and the SICGAT architecture [5] (right). Note that, apart from the main self-attention encoding layer, the adjacency graph masking and the fact that SICGAT compresses all input through averaging the channel information of the superpixel instead of having access to all pixels, both architectures are remarkably similar.

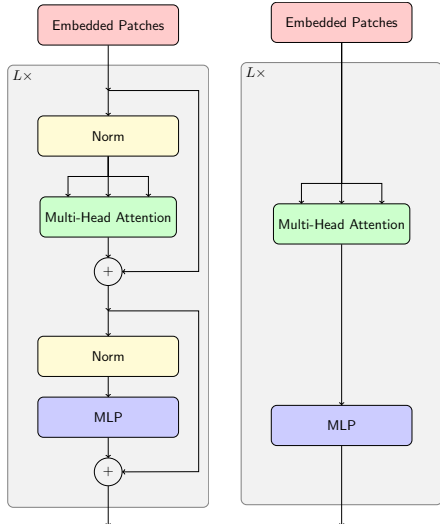


Figure 2: The Transformer Encoder [38] used on the ViT model [16] (left) and an equivalent view of a GAT encoder [39] used on the SICGAT model [5] (right). Using an attention mask on a transformer encoder would then be equivalent to using an adjacency matrix on a GAT encoder, with the only exception being the inner normalisation layers and residual connections.

tween these approaches is how positional information is treated. Earlier superpixel image classification models such as MoNet used positional information only as a weighting factor when performing neighbourhood aggregation, simply using this information as an inductive bias for the network. SICGAT extended this by appending each node’s positional information to the node’s features, treating the positional information in the same way as its pixel information. ViTs follow similarly but with two major differences: first, instead of appending the positional information to the pixel information, ViTs follow the previous standard used by Transformers and sums the positional information with the pixel information; lastly, due to the fact that ViTs uses a fixed number of equidistant patches, it encodes the positional information directly through a patch’s index instead of as a transformation of its xy coordinates.

Architectural differences A GAT layer and a Transformer layer have significant differences in their architectural components, with GATs being, in a sense, a simpler form of a Transformer Layer, which can be seen in Figure 2. Firstly, The GAT layer using in SICGAT only performs multi-head attention

and immediately follows it with a linear/MLP block to update a node’s information. The transformer layer instead first norms information before either the multi-head attention or MLP blocks, and then uses a residual approach to update the information instead of directly editing it, which has been shown to be an easier problem to solve and, thus, more efficient parameter-wise.

Chunk Connectivity Another difference is how connectivity is handled. Many of the earlier works in Superpixel Image Classification followed the same connectivity scheme as done by MoNet: a KNN graph based on chunk position. SICGAT tested their architecture only on a more restricted version of the problem, using instead a Region Adjacency Graph (RAG), arguing that it was both a harder problem as well as being closed conceptually to a convolution block, since only chunks that were physically connected would be also connected in this scheme. ViTs eschew this altogether and treat the image as a fully connected graph, leaving for the attentional mechanism to route the information flow between chunks.

Pooling vs virtual classification node Finally, the last major difference between these two models is that, while SICGAT average-pools the information in all nodes before feeding it into a classification head, ViTs again followed the traditional Transformer approach of adding a virtual classification node, which is then passed to the classification head. This would be equivalent to adding a virtual graph node, which is also another commonly used way to perform graph classification in Graph Neural Networks. In this paper we will follow the original ViT paper and work mainly with the concept of the classification, however it is worthy of note that more recent papers claim better performance by classifying and pooling over every single patch instead [8].

With these differences in mind, we can then build a generalisation that allows for both models to be represented under the framework, which we’ll describe in the following sections.

4.2 The Superpixel Transformer Model

We define here our framework called Superpixel Transformers (SPT) (Figure 4), which are an attempt at generalising (mostly attentional) SIC models and bridging the gap between these models and Vision Transformers, which see use in mainstream computer vision. Our framework is composed of 6 steps di-

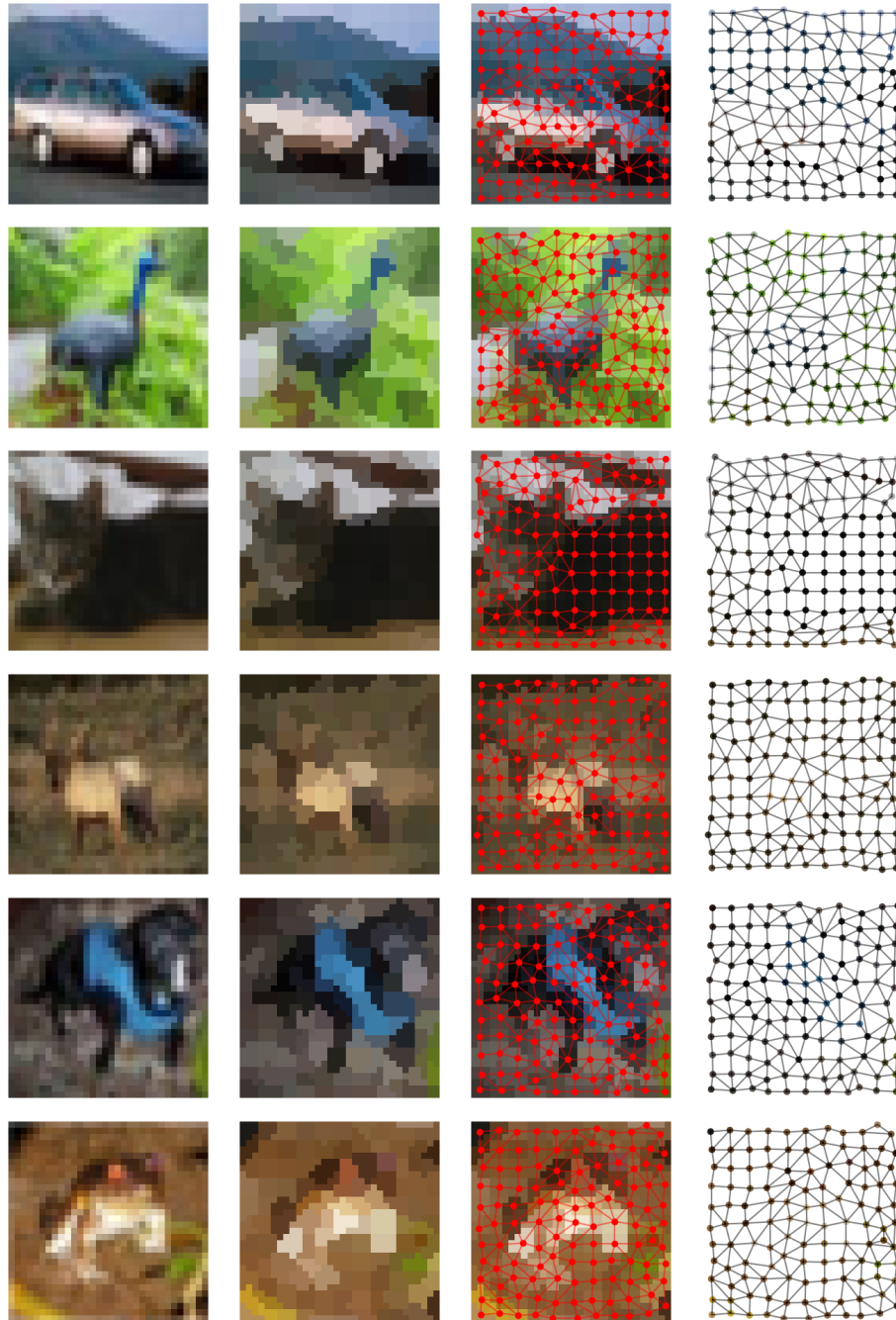


Figure 3: The information loss that happens when converting an image to a superpixel representation and then to its equivalent graph representation.

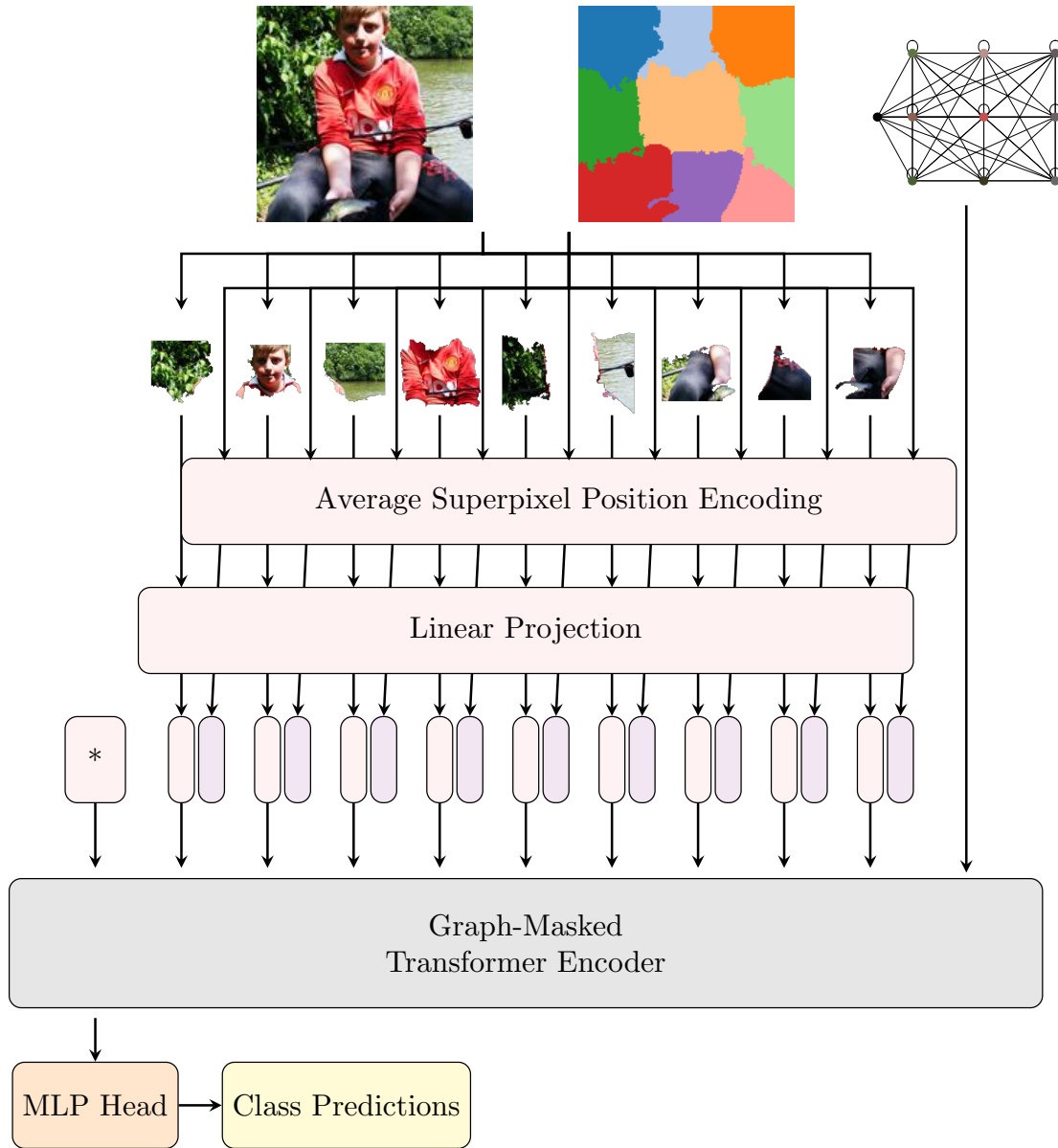


Figure 4: Our proposed Superpixel Transformer (SPT) architecture. Differently from SICGAT [5] we use the full superpixel information through the patch data structure built in Algorithm 1 and use a variety of superpixel positional encodings to build the input for our encoder network instead of encoding the position together with the patch information in the first GAT layer. Different from ViT [16] we allow for arbitrary superpixel algorithms and also use our model with a variety of adjacency graphs which constrain and help information flow better through the model. Also, due to the superpixel patches possibly having different shapes and positions, we extend and allow for encodings that use the xy coordinates of the superpixel/patch.

vided into preprocessing and on how to use the input for the network architecture. In the preprocessing stage, given an image I , we use a chunking strategy f_S to divide the image into its chunks/superpixels S that contain information about both the superpixel’s content S_c and its position S_p on the image, then we use a connectivity strategy f_G to build a connectivity graph G between the superpixels. Then, the superpixels S and input graph G are passed first encoded through a positional encoding strategy P and a content encoding strategy C , to be passed through a self-attention module (e.g. Transformer Encoder) that will finally be used to produce a classification. We’ll discuss the particular choices for each step below.

In the preprocessing part we choose two specific chunking strategies: A grid-based chunking (similar to what was done in [16]) that we define precisely in Algorithm A and which returns a $\mathbb{Z}^{h \times w}$ integer mask showing which superpixel each pixel belongs to, and SLIC0 [2, 1] (here onwards also referred to as SLIC), which provides a similar output but follows a spatiocontent kmeans variation to divide pixels into superpixels. Specifically, we used the implementation in `scikit-image` version 0.24. After obtaining the mask from a superpixel strategy, such as one of the two above, we use the segment mask to construct a neighbourhood graph G and use both the image and the segment mask into an algorithm that builds out superpixel patch data structure. The data structure we use is composed of three major components: An $\mathbb{R}^{k \times 2}$ tensor containing the xy positions of each superpixel, an $\mathbb{R}^{k \times 3 \times h_{chunk} \times w_{chunk}}$ tensor that contains the superpixel’s RGB content, and an $\{0, 1\}^{k \times 1 \times h_{chunk} \times w_{chunk}}$ mask that contains the superpixel’s shape content. We originally used a $h_{chunk} = w_{chunk} = k_{chunk} \times S$ with $k_{chunk} = 2$ since that is the search limit on the SLIC algorithm [2], but the SLIC implementation we used allowed superpixels with dimensions larger than $2S$, therefore we set $k_{chunk} = 3$. To allow for batching we provide a fixed-size superpixel chunk tensor, and thus we also provide a $\{0, 1\}^k$ mask to inform the transformer which chunks contain information. The full procedure to build this data structure can be seen in Algorithm 1. Note that while we define our model here for 2-dimensional data with 3 channels, it can easily be adapted to more dimensions and a different number of channels. For simplicity’s sake we transform any image with only a single channel to a 3-channel grayscale image.

For the graph-generation strategies we tested three strategies: 1. Using a fully connected graph `fcg`, similar to what a Vision Transformer uses [16]; 2. Using a graph build through a positional k-nearest neighbours `knn` [28]; 3. And using a Region-Adjacency graph `rag`, as defined in [5]. These strategies encompass most of the strategies used in previous models.

After producing our data structures it is then fed to our end-to-end model, which encode the chunk’s with single fully connected layer as is done with the original ViT [16]. Although our model can also be trained using convolutional stems [45], we do not do so for this paper. We test three different strategies for encoding a node’s position: 1. The original learned positional embedding used in the ViT [16] and proposed by [15]; 2. a simple Linear layer that maps the xy coordinates to the size of the embedding; and 3. an adaptation of the Sine-Cosine positional embedding originally used in [38], but expanded to work with multiple dimensions, the algorithm for which can be see in A. We then apply a transformer encoder network using the adjacency graph to define the attention mask, as well as an extra classification token added which connects to all other tokens. We chose the transformer encoder architecture instead of a GAT encoder due to both more mature Transformer implementations and the fact that the Transformer Encoder includes normalisation layers which are known to help stabilise training. Finally, we extract the classification token to pass on to a classification MLP.

5 Environment

We train all of our models from scratch, taking most of the hyperparameters from [34], with different values marked by *:

- Learning Rate: 1e-3
- Learning Rate Scheduler*: We Reduce the LR on a plateau by a factor of with a patience of 20% the number of epochs
- Dropout = 0.1
- Global Gradient Clipping = 1.0 for FashionMNIST and Imagenette
- Weight Decay: 1e-4
- Optimiser: Adam [24], using $\beta_1 = 0.9$ and $\beta_2 = 0.999$

Algorithm 1 Get Superpixel Patches

Require: image $\in \mathbb{R}^{C \times h \times w}$, segments $\in \mathbb{Z}^{h \times w}$, max_patches $\in \mathbb{Z}$, patch_shape $\in \mathbb{Z}^2$

Require: search_patch_size $\in \mathbb{Z}$, background_fill strategy

Ensure: spixpresent, spixcenters, spixpatches, spixpatchpresent

```
1: Initialize spixpresent, spixcenters, spixpatches, and spixpatchpresent if not provided
2: Fill spixpatches according to a background_fill strategy ▷ Default: all zeros
3: Mark segments with data: spixpresent[: segments.max() + 1]  $\leftarrow$  1
4: for  $i \leftarrow 0$  to segments.max() do
5:   spixpos  $\leftarrow$  positions where segments =  $i$ 
6:   spixmins, spixmaxs  $\leftarrow$  min(spixpos), max(spixpos)
7:   spixcenters[ $i$ ]  $\leftarrow$  spixmins +  $\frac{\text{spixmaxs} - \text{spixmins}}{2}$ 
8:    $y_0, x_0 \leftarrow \lfloor (\text{spixcenters}[i] - \frac{\text{search\_patch\_size}}{2}) \rfloor$ 
9:    $y_1, x_1 \leftarrow \lfloor (\text{spixcenters}[i] + \frac{\text{search\_patch\_size}}{2}) \rfloor$ 
10:  spixpos  $\leftarrow$  positions within box  $[y_0, y_1, x_0, x_1]$ 
11:  Update spixpatches by copying colour information from the  $i$ -th superpixel’s component pixels
12:  Update spixpatchpresent as a binary mask showing which pixels in spixpatches are contained in  $i$ -th
    the superpixel
13: end for
    return spixpresent, spixcenters, spixpatches, spixpatchpresent
```

- Due to instabilities on FashionMNIST, we do not backpropagate any batches that cause invalid gradients.

Due to compute constraints, we evaluate our models only on 4 datasets: FashionMNIST [44], CIFAR10 [26], Imagenette [22], and Resisc45 [12], which are described in Table 1. We have to limit the batch size, setting it as 512 for the MNIST and CIFAR10 datasets, 64 for the TinyImagenet and 32 for the Resisc dataset. We train Ti-sized models on all datasets except on Resisc45, where we train a B-sized model. We use $k=15$ for all KNN graphs. Whenever a superpixel would violate a patch’s bounds, we clip it to fit the patch by keeping the centermost pixels, and we used patch of size $3 \times S$.

6 Results

We trained Ti-sized models [34] using all combinations of graph connectivity strategies, patch building strategies, and superpixel building strategy, for 7 possible layer sizes: 1, 2, 4, 6, 8, 10, and 12. The layer size which provided the best validation accuracy out of the 7 test is shown for each of the combinations in Table 3 and in 5. The best result of the SLIC-based model from this table is shown in 2 as our model, even though we had a better performing model using the grid superpixel generation strategy. The ViT model (Grid-BERT-fcg combination)

achieved a slightly higher but comparable validation performance to our best SLIC model on the CIFAR10 dataset and a slightly lower but comparable performance in the FashionMNIST dataset.

Our proposed graph connectivity strategies also boosted the validation performance of the Grid-based superpixel models when compared to the fully connected graphs, and all of our trained models (including the ViT) outperformed the Graph Superpixel Image Classification baselines in all datasets. We trained an SPT-Ti (12 layers, Sine-Cosine, fcg) and a ViT-Ti (12 layers, BERT, fcg) model on the Imagenette dataset to provide a result for which the image was not too small, and both models were comparable and, while no previous SIC work has provided results on higher-resolution images, we believe that due the information loss shown in [5] would make it very hard for these models to perform anywhere close to our models.

We trained our SPT-B model with patch size of $S \approx 10$ for about 150 on the Resisc45 dataset using a NVIDIA GTX 1070m, after which it achieved a validation accuracy of 53.5%, which only slightly lower performance to that reported for the much larger ViT-B with a patch size of 16 trained from scratch for a similar amount of hours on a higher-end GPU. When testing our model on the Imagenette dataset a SLIC-based Ti model with Sine-Cosine positional embedding achieved 67.7% test accuracy while a grid-based Sine-Cosine model achieved 67.3%.

Dataset	Training	Validation	Test	Total	C,W,H	#Classes	S
FashionMNIST [44]	*54,000	*6,000	10,000	70,000	1, 28, 28	10	4
CIFAR10[26]	*47,500	*2,500	10,000	60,000	3,32,32	10	4
Imagenette [14, 22]	*8,996	*473	3,925	13,394	3, 160, 160	10	10
Resisc45 [12]	28350	3150	†	31500	3, 256, 256	45	10

Table 1: The description of the datasets used. C,W,H stand for the number of Channels, Width, and Height of the images. * Original development split was split randomly into train and validation, † No test set provided, results are shown for validation

Model	FashionMNIST		CIFAR10		Imagenette	
	Valid	Test	Valid	Test	Valid	Test
VGG-16 [36]	-	92.0	-	77.2	83.3	83.5
VGG-16 SLIC [5]	-	-	-	62.9	-	-
SICGAT [5]	-	83.1	53.4	45.9	-	-
gSLICr-GCN (l=12) [36]	-	81.9	-	59.5	-	-
bestGCN [30]	-	84.2	-	58.5	-	-
ViT [16] (our results)	86.5	<u>85.6</u>	70.6	69.0	-	67.9
SPT-slic (ours)	87.9	87.3	67.0	<u>63.3</u>	-	<u>67.7</u>

Table 2: Results for the three main datasets we tested our models in. Due to compute limitations we did not re-train models and instead use other author’s claimed results. For our models we limit ourselves to using only SPT models using SLIC superpixels and we use the test results of whichever model provided the best valid accuracy in our ablation study. For the ViT model we only consider its original implementation’s hyperparameters: Fully-connected graph with a BERT embedding. For the Imagenette result we use fully connected graphs with the Sine-Cosine positional embedding. For the VGG-16 architecture we use results reported in [36, 27, 23].

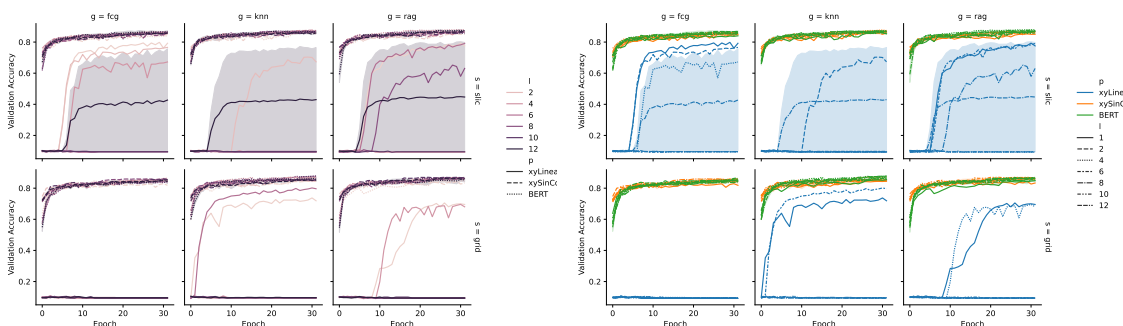


Figure 5: Plots highlighting the Validation Accuracy throughout the epochs for all the configurations we trained on the FashionMNIST dataset. One can see from graph on the left that the number of layers seemed to have little to no impact for the FashionMNIST dataset, except for the Linear positional embedding based on the xy coordinates. From the graph on the right it’s possible to see that the Linear embedding caused an extremely unstable training and sometimes even failed to reach similar accuracy levels.

S	P	G	Valid Acc (%)		Epochs		Layers	
			Best	Last	Best	Last		
FashionMNIST								
SLIC	Linear	fcg	80.0	79.2	30	32	1	
		knn	77.2	76.5	28	32	12	
		rag	80.2	79.8	31	32	12	
	SinCos	fcg	86.3	86.3	32	32	6	
		knn	87.7	87.4	31	32	4	
		rag	87.0	87.0	32	32	12	
	BERT	fcg	87.4	87.3	25	32	12	
		knn	87.5	87.5	32	32	12	
		rag	*87.9	87.8	31	32	4	
	Grid	Linear	fcg	10.9	9.5	3	32	6
			knn	80.2	79.6	31	32	6
			rag	70.5	69.5	27	32	1
SinCos		fcg	86.0	85.9	24	32	8	
		knn	87.2	87.2	32	32	4	
		rag	87.0	86.8	23	32	10	
BERT		fcg	†86.5	86.5	32	32	2	
		knn	<u>*87.9</u>	87.9	32	32	8	
		rag	87.2	87.2	31	32	2	
CIFAR10								
SLIC		SinCos	fcg	*67.0	64.4	221	279	10
			knn	67.0	65.7	185	187	2
	rag		66.4	65.0	279	308	4	
	BERT	fcg	60.8	59.9	162	271	6	
		knn	61.9	59.6	172	198	10	
		rag	65.2	64.2	504	506	4	
Grid	SinCos	fcg	70.8	69.4	388	418	10	
		knn	72.2	71.8	450	475	12	
		rag	<u>74.3</u>	73.1	272	420	8	
	BERT	fcg	†70.6	69.5	479	512	6	
		knn	71.7	69.5	253	260	6	
		rag	*75.5	72.2	492	512	8	

Table 3: Ablation Study for each superpixel generation strategy S , each positional embedding P , and each graph connectivity strategy G for the FashionMNIST and CIFAR10 datasets. We mark the **best** and second best validation accuracies for each dataset. The best SLIC-based model and non-ViT grid-based is marked with *, and the original ViT model is marked with †. For the CIFAR10 dataset Linear embeddings were failing and thus were cancelled to save compute time.

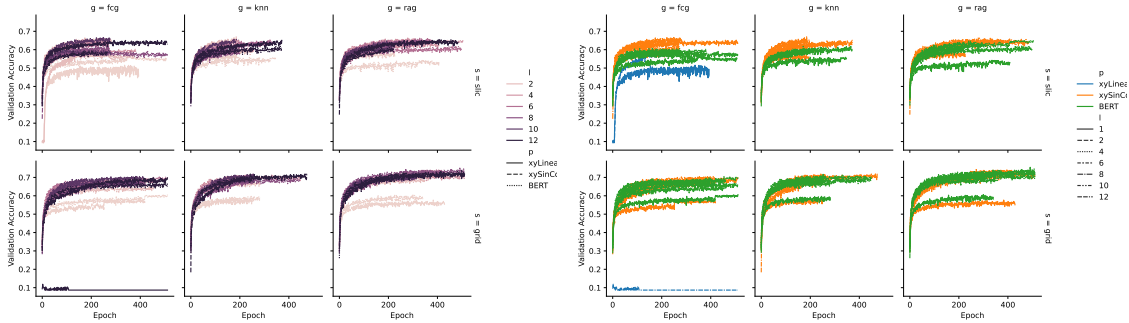


Figure 6: Plots highlighting the Validation Accuracy throughout the epochs for all the configurations we trained on the CIFAR10 dataset. One can see from graph on the left that the number of layers seemed to be more relevant for this dataset than the FashionMNIST dataset, possibly due to this dataset requiring a higher model capacity. Higher numbers of layers, however, often had a diminishing returns effect and sometime even negatively affected performance. For the slic model, the BERT encoding often fared worse than the Sine-Cosine embedding based on the xy coordinates. This is likely due to the fact that the superpixel embeddings have variable xy coordinates and thus the fixed learned positional encoding cannot work properly. Due to resource-sharing on HPC many models ran for fewer epochs, an analysis of time complexity and time per iteration can be see in Table A1 and Figure A1 where we analyse based on the FashionMNIST dataset, which ran on a more controlled environment. The linear xy positional embedding exhibited inconsistent performance and was dropped from further experiments early on.

7 Conclusion

In this paper we proposed a generalisation of the Vision Transformer model to accept arbitrary superpixel formats and graph connectivities, bridging the gap between using Vision Transformers and the Superpixel-based Image Classification literature. We’ve tested our models with two different Superpixel generation strategies, three graph connectivity strategies, and three positional embedding strategies, showing through this ablation study that our proposed multidimensional SinCos worked better for both, and that graph connectivity strategies produce different results in different datasets.

Furthermore, we validated our model against three previous works on Superpixel Image Classification and show better performance than these baselines, showing that even when constrained to working under a superpixel framework (e.g. if one wants to transfer between euclidean and non-euclidean images as was proposed in [5], one could use a similar approach to ours and would only need to adapt the initial embedding head, keeping the transformer core of the model. We test our model on datasets with different image sizes and sample contents, showing that our model can adapt to these different circumstances.

Our model, however, does not come without com-

promises. To be able to fully utilise the superpixel information an extra channel was needed during the patch embedding and the lack of search distance limitations on the SLIC implementation used meant that our patches could have sizes above the $2S$ limit defined in the original SLIC/SLIC0 algorithm [2]. Furthermore, since the number of superpixels is dynamic and might be different than the value specified, it was necessary to provide padding on the input sequences. These issues, however, did not constitute a major resource consumption increase in our model. Our experiments were also heavily limited due to the compute available to us, which we hope to overcome on future work with access to better compute.

Future work can address some of the abovementioned weaknesses of our models and can also attempt to use convolutional cores in the patch embedding heads [45], as these would allow the model to better identify the superpixel’s component parts and take full advantage of the superpixel’s shape and colour information. Finally, future work could also focus on pre-training a Superpixel-based model, since pre-training is known to be a much better strategy for training transformer-based image models [34], this would also allow one to attempt transferring models between euclidean and non-euclidean domains as mentioned above, which our model is naturally more

suitable for due to its flexible learning pattern, even though our results are only comparable to a standard ViT model.

Acknowledgements

This work was partially funded by CAPES Finance code (001) and CNPq. Some of the HPC used in this work was funded by Petrobras call TC 5900.0111175.19.9, 2020/00182-5, and FAPERGS call 16/2551-0000348-8 to Lucas Melo Schnorr. Some experiments in this work used the PCAD infrastructure, <http://gppd-hpc.inf.ufrgs.br>, at INF/UFRGS. We would like to thank Dylan Alexander Slavin Hillier for his help proofreading this paper.

Authors' contributions

PHdCA did experiment and model design, implementation, and execution, and wrote and reviewed the article. ART and LCL, interacted in discussions, wrote, and reviewed the article.

References

- [1] R. Achanta, A. Shaji, K. Smith, A. Lucchi, P. Fua, and Sabine Süssstrunk. SLIC Superpixels Compared to State-of-the-Art Superpixel Methods. *IEEE Transactions on Pattern Analysis and Machine Intelligence*, 34(11):2274–2282, November 2012.
- [2] Radhakrishna Achanta, Appu Shaji, Kevin Smith, Aurelien Lucchi, Pascal Fua, and Sabine Süssstrunk. SLIC Superpixels: SLICO, June 2010.
- [3] Radhakrishna Achanta and Sabine Susstrunk. Superpixels and Polygons Using Simple Non-iterative Clustering. In *2017 IEEE Conference on Computer Vision and Pattern Recognition (CVPR)*, pages 4895–4904, Honolulu, HI, July 2017. IEEE.
- [4] Pedro Avelar, Henrique Lemos, Marcelo Prates, and Luis Lamb. Multitask Learning on Graph Neural Networks: Learning Multiple Graph Centrality Measures with a Unified Network. In Igor V. Tetko, Věra Kůrková, Pavel Karpov, and Fabian Theis, editors, *Artificial Neural Networks and Machine Learning – ICANN 2019: Workshop and Special Sessions*, volume 11731, pages 701–715. Springer International Publishing, Cham, 2019. Series Title: Lecture Notes in Computer Science.
- [5] Pedro H. C. Avelar, Anderson R. Tavares, Thiago L. T. da Silveira, Cláudio R. Jung, and Luis C. Lamb. Superpixel Image Classification with Graph Attention Networks. In *2020 33rd SIBGRAPI Conference on Graphics, Patterns and Images (SIBGRAPI)*, pages 203–209, Recife/Porto de Galinhas, Brazil, November 2020. IEEE.
- [6] Dzmitry Bahdanau, Kyunghyun Cho, and Yoshua Bengio. Neural Machine Translation by Jointly Learning to Align and Translate. In Yoshua Bengio and Yann LeCun, editors, *3rd International Conference on Learning Representations, ICLR 2015, Conference Track Proceedings*, San Diego, CA, USA., May 2015.
- [7] Peter W. Battaglia, Jessica B. Hamrick, Victor Bapst, Alvaro Sanchez-Gonzalez, Vinicius Zambaldi, Mateusz Malinowski, Andrea Tacchetti, David Raposo, Adam Santoro, Ryan Faulkner, Caglar Gulcehre, Francis Song, Andrew Ballard, Justin Gilmer, George Dahl, Ashish Vaswani, Kelsey Allen, Charles Nash, Victoria Langston, Chris Dyer, Nicolas Heess, Daan Wierstra, Pushmeet Kohli, Matt Botvinick, Oriol Vinyals, Yujia Li, and Razvan Pascanu. Relational inductive biases, deep learning, and graph networks, October 2018. arXiv:1806.01261 [cs, stat].
- [8] Lucas Beyer, Xiaohua Zhai, and Alexander Kolesnikov. Better plain ViT baselines for ImageNet-1k, May 2022. arXiv:2205.01580 [cs].
- [9] M. Bianchini, M. Maggini, L. Sarti, and F. Scarselli. Recursive neural networks learn to localize faces. *Pattern Recognition Letters*, 26(12):1885–1895, September 2005.
- [10] Shaked Brody, Uri Alon, and Eran Yahav. How Attentive are Graph Attention Networks? In *The Tenth International Conference on Learning Representations, ICLR 2022*, Virtual Event, April 2022. OpenReview.net.
- [11] Jiawei Chen, Hao Xu, Wanyu Tao, Zhaoxiong Chen, Yuxuan Zhao, and Jing-Dong J. Han. Transformer for one stop interpretable cell type annotation. *Nature Communications*, 14(1):223, January 2023.

- [12] Gong Cheng, Junwei Han, and Xiaoqiang Lu. Remote Sensing Image Scene Classification: Benchmark and State of the Art. *Proceedings of the IEEE*, 105(10):1865–1883, October 2017.
- [13] Haotian Cui, Chloe Wang, Hassaan Maan, Kuan Pang, Fengning Luo, and Bo Wang. scGPT: Towards Building a Foundation Model for Single-Cell Multi-omics Using Generative AI. preprint, *Bioinformatics*, May 2023.
- [14] Jia Deng, Wei Dong, Richard Socher, Li-Jia Li, Kai Li, and Li Fei-Fei. ImageNet: A large-scale hierarchical image database. In *2009 IEEE Conference on Computer Vision and Pattern Recognition*, pages 248–255, Miami, FL, June 2009. IEEE.
- [15] Jacob Devlin, Ming-Wei Chang, Kenton Lee, and Kristina Toutanova. BERT: Pre-training of Deep Bidirectional Transformers for Language Understanding. In Jill Burstein, Christy Doran, and Thamar Solorio, editors, *Proceedings of the 2019 Conference of the North American Chapter of the Association for Computational Linguistics: Human Language Technologies, NAACL-HLT 2019*, volume 1, pages 4171–4186, Minneapolis, MN, USA, July 2019. Association for Computational Linguistics.
- [16] Alexey Dosovitskiy, Lucas Beyer, Alexander Kolesnikov, Dirk Weissenborn, Xiaohua Zhai, Thomas Unterthiner, Mostafa Dehghani, Matthias Minderer, Georg Heigold, Sylvain Gelly, Jakob Uszkoreit, and Neil Houlsby. An Image is Worth 16x16 Words: Transformers for Image Recognition at Scale. In *9th International Conference on Learning Representations, ICLR 2021*, Virtual Event, Austria, May 2021. OpenReview.net.
- [17] Vijay Prakash Dwivedi and Xavier Bresson. A Generalization of Transformer Networks to Graphs, January 2021. arXiv:2012.09699 [cs].
- [18] Matthias Fey, Jan Eric Lenssen, Frank Weichert, and Heinrich Muller. SplineCNN: Fast Geometric Deep Learning with Continuous B-Spline Kernels. In *2018 IEEE/CVF Conference on Computer Vision and Pattern Recognition*, pages 869–877, Salt Lake City, UT, June 2018. IEEE.
- [19] Justin Gilmer, Samuel S. Schoenholz, Patrick F. Riley, Oriol Vinyals, and George E. Dahl. Neural Message Passing for Quantum Chemistry. In Doina Precup and Yee Whye Teh, editors, *Proceedings of the 34th International Conference on Machine Learning, ICML 2017*, volume 70 of *Proceedings of Machine Learning Research*, pages 1263–1272, Sydney, NSW, Australia, August 2017. PMLR.
- [20] Alex Graves, Santiago Fernández, and Jürgen Schmidhuber. Bidirectional LSTM Networks for Improved Phoneme Classification and Recognition. In Włodzisław Duch, Janusz Kacprzyk, Erkki Oja, and Sławomir Zadrozny, editors, *Artificial Neural Networks: Formal Models and Their Applications - ICANN 2005, 15th International Conference, Warsaw, Poland, September 11-15, 2005, Proceedings, Part II*, volume 3697 of *Lecture Notes in Computer Science*, pages 799–804, Warsaw, Poland, September 2005. Springer.
- [21] Shion Honda, Shoi Shi, and Hiroki R. Ueda. SMILES Transformer: Pre-trained Molecular Fingerprint for Low Data Drug Discovery. 2019. Publisher: arXiv Version Number: 1.
- [22] Jeremy Howard and Imagenette Contributors. fastai/imagenette, November 2024. original-date: 2019-03-06T01:58:45Z.
- [23] Kasen. VGG model construction and Imagenette image recognition based on PyTorch, September 2024.
- [24] Diederik P. Kingma and Jimmy Ba. Adam: A Method for Stochastic Optimization. In Yoshua Bengio and Yann LeCun, editors, *3rd International Conference on Learning Representations, ICLR 2015, San Diego, CA, USA, May 7-9, 2015, Conference Track Proceedings*, 2015.
- [25] Thomas N. Kipf and Max Welling. Semi-Supervised Classification with Graph Convolutional Networks. In *5th International Conference on Learning Representations, ICLR 2017, Conference Track Proceedings*, Toulon, France, April 2017. OpenReview.net.
- [26] Alex Krizhevsky. Learning multiple layers of features from tiny images. Master’s thesis, University of Toronto, Toronto, Canada, April 2009.

- [27] Shreyasi Mandal. VGG16 on MNIST and Fashion_mnist, November 2023.
- [28] Federico Monti, Davide Boscaini, Jonathan Masci, Emanuele Rodola, Jan Svoboda, and Michael M. Bronstein. Geometric Deep Learning on Graphs and Manifolds Using Mixture Model CNNs. In *2017 IEEE Conference on Computer Vision and Pattern Recognition (CVPR)*, pages 5425–5434, Honolulu, HI, July 2017. IEEE.
- [29] OpenAI, Josh Achiam, Steven Adler, Sandhini Agarwal, Lama Ahmad, Ilge Akkaya, Florencia Leoni Aleman, Diogo Almeida, Janko Altschmidt, Sam Altman, Shyamal Anadkat, Red Avila, Igor Babuschkin, Suchir Balaji, Valerie Balcom, Paul Baltescu, Haiming Bao, Mo Bavarian, Jeff Belgum, Irwan Bello, Jake Berdine, Gabriel Bernadett-Shapiro, Christopher Berner, Lenny Bogdonoff, Oleg Boiko, Madelaine Boyd, Anna-Luisa Brakman, Greg Brockman, Tim Brooks, Miles Brundage, Kevin Button, Trevor Cai, Rosie Campbell, Andrew Cann, Brittany Carey, Chelsea Carlson, Rory Carmichael, Brooke Chan, Che Chang, Fotis Chantzis, Derek Chen, Sully Chen, Ruby Chen, Jason Chen, Mark Chen, Ben Chess, Chester Cho, Casey Chu, Hyung Won Chung, Dave Cummings, Jeremiah Currier, Yunxing Dai, Cory Decareaux, Thomas Degry, Noah Deutsch, Damien Deville, Arka Dhar, David Dohan, Steve Dowling, Sheila Dunning, Adrien Ecoffet, Atty Eleti, Tyna Eloundou, David Farhi, Liam Fedus, Niko Felix, Simón Posada Fishman, Juston Forte, Isabella Fulford, Leo Gao, Elie Georges, Christian Gibson, Vik Goel, Tarun Gogineni, Gabriel Goh, Rapha Gontijo-Lopes, Jonathan Gordon, Morgan Grafstein, Scott Gray, Ryan Greene, Joshua Gross, Shixiang Shane Gu, Yufei Guo, Chris Hallacy, Jesse Han, Jeff Harris, Yuchen He, Mike Heaton, Johannes Heidecke, Chris Hesse, Alan Hickey, Wade Hickey, Peter Hoeschele, Brandon Houghton, Kenny Hsu, Shengli Hu, Xin Hu, Joost Huizinga, Shantanu Jain, Shawn Jain, Joanne Jang, Angela Jiang, Roger Jiang, Haozhun Jin, Denny Jin, Shino Jomoto, Billie Jonn, Heewoo Jun, Tomer Kaftan, Lukasz Kaiser, Ali Kamali, Ingmar Kanitscheider, Nitish Shirish Keskar, Tabarak Khan, Logan Kilpatrick, Jong Wook Kim, Christina Kim, Yongjik Kim, Hendrik Kirchner, Jamie Kiros, Matt Knight, Daniel Kokotajlo, Lukasz Kondraciuk, Andrew Kondrich, Aris Konstantinidis, Kyle Kosic, Gretchen Krueger, Vishal Kuo, Michael Lampe, Ikai Lan, Teddy Lee, Jan Leike, Jade Leung, Daniel Levy, Chak Ming Li, Rachel Lim, Molly Lin, Stephanie Lin, Mateusz Litwin, Theresa Lopez, Ryan Lowe, Patricia Lue, Anna Makanju, Kim Malfacini, Sam Manning, Todor Markov, Yaniv Markovski, Bianca Martin, Katie Mayer, Andrew Mayne, Bob McGrew, Scott Mayer McKinney, Christine McLeavey, Paul McMillan, Jake McNeil, David Medina, Aalok Mehta, Jacob Menick, Luke Metz, Andrey Mishchenko, Pamela Mishkin, Vinnie Monaco, Evan Morikawa, Daniel Mossing, Tong Mu, Mira Murati, Oleg Murk, David Mély, Ashvin Nair, Reiichiro Nakano, Rajeev Nayak, Arvind Neelakantan, Richard Ngo, Hyeonwoo Noh, Long Ouyang, Cullen O’Keefe, Jakub Pachocki, Alex Paino, Joe Palermo, Ashley Pantuliano, Giambattista Parascandolo, Joel Parish, Emy Parparita, Alex Passos, Mikhail Pavlov, Andrew Peng, Adam Perelman, Filipe de Avila Belbute Peres, Michael Petrov, Henrique Ponde de Oliveira Pinto, Michael, Pokorny, Michelle Pokrass, Vitchyr Pong, Tolly Powell, Alethea Power, Boris Power, Elizabeth Proehl, Raul Puri, Alec Radford, Jack Rae, Aditya Ramesh, Cameron Raymond, Francis Real, Kendra Rimbach, Carl Ross, Bob Rotsted, Henri Roussez, Nick Ryder, Mario Saltarelli, Ted Sanders, Shibani Santurkar, Girish Sastry, Heather Schmidt, David Schnurr, John Schulman, Daniel Selsam, Kyla Sheppard, Toki Sherbakov, Jessica Shieh, Sarah Shoker, Pranav Shyam, Szymon Sidor, Eric Sigler, Maddie Simens, Jordan Sitkin, Katarina Slama, Ian Sohl, Benjamin Sokolowsky, Yang Song, Natalie Staudacher, Felipe Petroski Such, Natalie Summers, Ilya Sutskever, Jie Tang, Nikolas Tezak, Madeleine Thompson, Phil Tillet, Amin Tootoonchian, Elizabeth Tseng, Preston Tuggle, Nick Turley, Jerry Tworek, Juan Felipe Cerón Uribe, Andrea Vallone, Arun Vijayvergiya, Chelsea Voss, Carroll Wainwright, Justin Jay Wang, Alvin Wang, Ben Wang, Jonathan Ward, Jason Wei, C. J. Weinmann, Akila Welihinda, Peter Welinder, Jiayi Weng, Lilian Weng, Matt Wiethoff, Dave Willner, Clemens Winter, Samuel Wolrich, Hannah Wong, Lauren Workman, Sherwin Wu, Jeff Wu, Michael Wu, Kai Xiao, Tao Xu, Sarah Yoo, Kevin Yu, Qiming

- Yuan, Wojciech Zaremba, Rowan Zellers, Chong Zhang, Marvin Zhang, Shengjia Zhao, Tianhao Zheng, Juntang Zhuang, William Zhuk, and Barret Zoph. GPT-4 Technical Report, December 2023. arXiv:2303.08774 [cs].
- [30] Júlia Rodrigues and Joel Carbonera. Graph Convolutional Networks for Image Classification: Comparing Approaches for Building Graphs from Images. In *Proceedings of the 26th International Conference on Enterprise Information Systems*, volume 1, pages 437–446, Angers, France, 2024. SCITEPRESS - Science and Technology Publications.
- [31] F. Scarselli, M. Gori, Ah Chung Tsoi, M. Hagenbuchner, and G. Monfardini. The Graph Neural Network Model. *IEEE Transactions on Neural Networks*, 20(1):61–80, January 2009.
- [32] M. Schuster and K.K. Paliwal. Bidirectional recurrent neural networks. *IEEE Transactions on Signal Processing*, 45(11):2673–2681, November 1997.
- [33] Daniel Selsam, Matthew Lamm, Benedikt Bünz, Percy Liang, Leonardo de Moura, and David L. Dill. Learning a SAT Solver from Single-Bit Supervision. In *7th International Conference on Learning Representations, ICLR 2019, New Orleans, LA, USA, May 6-9, 2019*, New Orleans, LA, USA, May 2019. OpenReview.net.
- [34] Andreas Peter Steiner, Alexander Kolesnikov, Xiaohua Zhai, Ross Wightman, Jakob Uszkoreit, and Lucas Beyer. How to train your ViT? Data, Augmentation, and Regularization in Vision Transformers. *Transactions on Machine Learning Research*, 2022.
- [35] David Stutz, Alexander Hermans, and Bastian Leibe. Superpixels: An evaluation of the state-of-the-art. *Computer Vision and Image Understanding*, 166:1–27, January 2018.
- [36] Tinglong Tang, Xiaowang Chen, Yirong Wu, Shuifa Sun, and Mei Yu. Image Classification Based on Deep Graph Convolutional Networks. In *2022 IEEE 9th International Conference on Data Science and Advanced Analytics (DSAA)*, pages 1–6, Shenzhen, China, October 2022. IEEE.
- [37] Michael Van Den Bergh, Xavier Boix, Gemma Roig, Benjamin De Capitani, and Luc Van Gool. SEEDS: Superpixels Extracted via Energy-Driven Sampling. In David Hutchison, Takeo Kanade, Josef Kittler, Jon M. Kleinberg, Friedemann Mattern, John C. Mitchell, Moni Naor, Oscar Nierstrasz, C. Pandu Rangan, Bernhard Steffen, Madhu Sudan, Demetri Terzopoulos, Doug Tygar, Moshe Y. Vardi, Gerhard Weikum, Andrew Fitzgibbon, Svetlana Lazebnik, Pietro Perona, Yoichi Sato, and Cordelia Schmid, editors, *Computer Vision – ECCV 2012*, volume 7578, pages 13–26. Springer Berlin Heidelberg, Berlin, Heidelberg, 2012. Series Title: Lecture Notes in Computer Science.
- [38] Ashish Vaswani, Noam Shazeer, Niki Parmar, Jakob Uszkoreit, Llion Jones, Aidan N. Gomez, Lukasz Kaiser, and Illia Polosukhin. Attention is All you Need. In Isabelle Guyon, Ulrike von Luxburg, Samy Bengio, Hanna M. Wallach, Rob Fergus, S. V. N. Vishwanathan, and Roman Garnett, editors, *Advances in Neural Information Processing Systems 30: Annual Conference on Neural Information Processing Systems 2017, December 4-9, 2017, Long Beach, CA, USA*, pages 5998–6008, 2017.
- [39] Petar Velickovic, Guillem Cucurull, Arantxa Casanova, Adriana Romero, Pietro Liò, and Yoshua Bengio. Graph Attention Networks. In *6th International Conference on Learning Representations, ICLR 2018, Vancouver, BC, Canada, April 30 - May 3, 2018, Conference Track Proceedings*, Vancouver, BC, Canada, May 2018. OpenReview.net.
- [40] Oriol Vinyals, Meire Fortunato, and Navdeep Jaitly. Pointer Networks. In Corinna Cortes, Neil D. Lawrence, Daniel D. Lee, Masashi Sugiyama, and Roman Garnett, editors, *Advances in Neural Information Processing Systems 28: Annual Conference on Neural Information Processing Systems 2015, December 7-12, 2015, Montreal, Quebec, Canada*, pages 2692–2700, 2015.
- [41] Sheng Wang, Yuzhi Guo, Yuhong Wang, Hongmao Sun, and Junzhou Huang. SMILES-BERT: Large Scale Unsupervised Pre-Training for Molecular Property Prediction. In *Proceedings of the 10th ACM International Conference on Bioinformatics, Computational Biology and Health Informatics*, pages 429–436, Niagara Falls NY USA, September 2019. ACM.

- [42] Xing Wei, Qingxiong Yang, Yihong Gong, Narendra Ahuja, and Ming-Hsuan Yang. Super-pixel Hierarchy. *IEEE Transactions on Image Processing*, 27(10):4838–4849, October 2018.
- [43] Fang Wu, Dragomir Radev, and Stan Z. Li. Mol-former: Motif-Based Transformer on 3D Heterogeneous Molecular Graphs. *Proceedings of the AAAI Conference on Artificial Intelligence*, 37(4):5312–5320, June 2023.
- [44] Han Xiao, Kashif Rasul, and Roland Vollgraf. Fashion-MNIST: a Novel Image Dataset for Benchmarking Machine Learning Algorithms, September 2017. arXiv:1708.07747 [cs, stat].
- [45] Tete Xiao, Mannat Singh, Eric Mintun, Trevor Darrell, Piotr Dollár, and Ross B. Girshick. Early Convolutions Help Transformers See Better. In Marc’Aurelio Ranzato, Alina Beygelzimer, Yann N. Dauphin, Percy Liang, and Jennifer Wortman Vaughan, editors, *Advances in Neural Information Processing Systems 34: Annual Conference on Neural Information Processing Systems 2021, NeurIPS 2021, December 6-14, 2021, virtual*, pages 30392–30400, December 2021.
- [46] Keyulu Xu, Weihua Hu, Jure Leskovec, and Stefanie Jegelka. How Powerful are Graph Neural Networks? In *7th International Conference on Learning Representations, ICLR 2019, New Orleans, LA, USA, May 6-9, 2019*, New Orleans, LA, USA, May 2019. OpenReview.net.
- [47] Jian Yao, Marko Boben, Sanja Fidler, and Raquel Urtasun. Real-time coarse-to-fine topologically preserving segmentation. In *2015 IEEE Conference on Computer Vision and Pattern Recognition (CVPR)*, pages 2947–2955, Boston, MA, USA, June 2015. IEEE.

Appendix A

Algorithm A1 Square Grid Superpixel

Require: image $\in \mathbb{R}^{C \times h \times w}$, patch_size $\in \mathbb{Z}$

Ensure: segments $\in \mathbb{Z}^{h \times w}$

Ensure: $\sqrt{\text{n_segments}} \in \mathbb{Z}$

Ensure: $H \bmod \text{patch_size} = 0$

Ensure: $H = W$

```

1: num_patches_per_line  $\leftarrow \sqrt{\text{n\_segments}}$ 
2: Initialize segments  $\leftarrow \text{zeros}(H, W)$ 
3: for  $i \leftarrow 0$  to  $\text{n\_segments} - 1$  do
4:    $i_y \leftarrow \lfloor i / \text{num\_patches\_per\_line} \rfloor$ 
5:    $i_x \leftarrow i \bmod \text{num\_patches\_per\_line}$ 
6:   Assign segment index  $i$  to region in segments
7:   segments[ $i_y \times \text{patch\_size} \dots (i_y + 1) \times \text{patch\_size}, i_x \times \text{patch\_size} \dots (i_x + 1) \times \text{patch\_size}$ ]  $\leftarrow i$ 
8: end for
9: return segments

```

Algorithm A2 Sine-Cosine Coordinate Encoding

Require: hidden_dim $\in \mathbb{Z}$, n_axes $\in \mathbb{Z}$

Ensure: pos_emb $\in \mathbb{R}^{b \times s \times h}$, where b is batch size, s is sequence length, h is hidden dimension

```

1: Initialize div_term =  $\exp([0 \dots h] \cdot (-\log(10000)/h))$ 
2: Initialize mixer =  $W \in \mathbb{R}^{h \times h}$ 
3: procedure ENCODE(pos, x)  $\triangleright$  pos is  $\mathbb{R}^{b \times s \times d}$ , x is  $\mathbb{R}^{b \times s \times h}$ 
4:    $d \leftarrow \min(\text{n\_axes}, \text{pos.shape}[2])$ 
5:   Initialize pos_emb  $\leftarrow \text{zeros\_like}(x)$ 
6:   for  $i \leftarrow 0$  to  $d - 1$  do  $\triangleright$  Build sin-cos for each dimension
7:     Select all indices for cosine as  $j_{\text{cos}} = \{i, i + 2d, i + 4d, \dots\}$  up to  $h$ 
8:     Select all indices for sine as  $j_{\text{sin}} = \{i + 1, i + 1 + 2d, i + 1 + 4d, \dots\}$  up to  $h$ 
9:     pos_emb[:, :,  $j_{\text{cos}}$ ]  $\leftarrow \cos(\text{pos}[:, :, i] \cdot \text{div\_term}[j_{\text{cos}}])$ 
10:    pos_emb[:, :,  $j_{\text{sin}}$ ]  $\leftarrow \sin(\text{pos}[:, :, i] \cdot \text{div\_term}[j_{\text{sin}}])$ 
11:   end for
12:   return mixer(pos_emb)
13: end procedure

```

S	P	G	$\mu(b)$	$\sigma(b)$		
slic	xyLinear	fcg	2191.445	79.985		
		xySinCos	2163.883	56.462		
		BERT	2163.673	91.721		
	xyLinear	rag	3018.270	67.750		
		xySinCos	2890.867	59.136		
		BERT	2945.360	97.905		
	grid	xyLinear	knn	3665.725	59.916	
			xySinCos	3784.874	75.899	
			BERT	3622.777	38.381	
xyLinear		fcg	2308.859	53.799		
		xySinCos	2198.941	40.184		
		BERT	2127.548	68.252		
slic		xyLinear	rag	2927.251	51.175	
			xySinCos	2820.486	32.625	
			BERT	2860.717	70.748	
	xyLinear	knn	3547.717	97.029		
		xySinCos	3590.628	77.070		
		BERT	3636.872	133.942		
	slic	xyLinear	*	2958.480	252.643	
			xySinCos	*	2946.541	274.293
			BERT	*	2910.603	244.672
grid	xyLinear	*	2927.942	251.979		
		xySinCos	*	2870.018	252.923	
		BERT	*	2875.046	261.837	
slic	*	fcg	2173.000	40.673		
		rag	2951.499	42.239		
		knn	3691.125	43.873		
grid	*	fcg	2211.783	35.102		
		rag	2869.485	30.399		
		knn	3591.739	56.513		
*	fcg	xyLinear	2250.152	52.541		
		xySinCos	2181.412	40.801		
		BERT	2145.611	54.348		
	rag	xyLinear	2972.761	45.539		
		xySinCos	2855.677	40.709		
		BERT	2903.039	66.223		
	knn	xyLinear	3606.721	55.538		
		xySinCos	3687.751	71.164		
		BERT	3629.824	65.661		
slic	*	*	2938.542	144.431		
grid	*	*	2891.002	143.395		
*	xyLinear	*	2943.211	174.740		
		xySinCos	*	2908.280	183.329	
		BERT	*	2892.825	175.366	
	*	fcg	2192.391	28.569		
		rag	2910.492	29.785		
		knn	3641.432	36.430		

Table A1: Table showing the average and standard deviation of the intercepts for linear regression models build on a certain combination of Superpixel, Positional Embedding and Graph Adjacency method. We can see that the Graph Adjacency method has the biggest impact on performance. Values for slopes are not included since most slopes had a non-significant p-value, and the comparison between intercepts yielded more significant p-values.

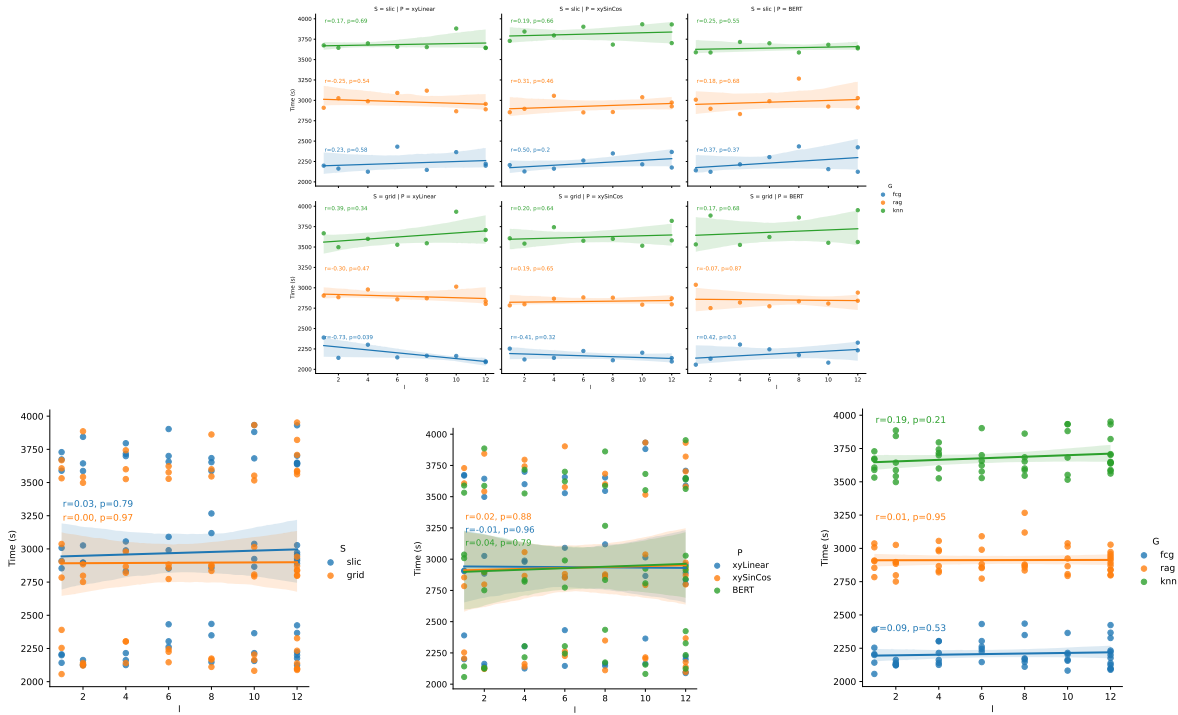


Figure A1: Figures showing regression plots (with person r and p values) between the number of layers and the time taken for the process to finish training and testing. The top figure shows results separated by each of the variables, and most results show a positive r but a not-significant p, with the only significant p having a negative r, which we believe to be spurious. Only when we look at each variable individually on the bottom figures that we are able to find significant differences between variables, and the graph building algorithm is has the biggest difference.